

Frequency characteristics of the complex permeability and its application to the FEM solutions of hysteretic fields

S. Hayano, A. Miyazaki, and Y. Saito

College of Engineering, Hosei University, Kajino, Koganei, Tokyo 184, Japan

A complex permeability is derived from a Chua-type magnetization model. The frequency characteristic of the complex permeability is calculated and compared with those of experiments. This complex permeability is applied to obtain the finite-element solutions of hysteretic fields. Examination of the field distributions suggests that the frequency characteristic of the magnetic materials is mainly dominated by the essential feature of complex permeability not the field distribution effects such as a skin effect.

I. INTRODUCTION

In order to realize small size power supplies, it is essential to increase the operating frequency of the magnetic devices, e.g., transformer and reactor. At high-frequency exciting conditions, the peak flux density in the magnetic materials is sufficiently small that both the flux density and field intensity are sinusoidally time varying. This makes it possible to employ a complex permeability representation of the magnetization characteristics. Previously, we have proposed a Chua-type magnetization model based on the magnetic domain theory.¹⁻⁵ Also, it has been shown that this Chua-type model is capable of representing the typical magnetization characteristics such as the aftereffect, minor loops, and ferroresonance phenomenon. In the present paper, the Chua-type model is now applied to derive a complex permeability. The frequency characteristic of this complex permeability is carefully examined by comparing it with the experimental results. Further, in order to examine the effects of hysteresis on the magnetic field distributions, the complex permeability is used to obtain the finite-element solutions of hysteretic fields. Examination of the field distributions suggests that the frequency characteristic of the magnetic materials is mainly dominated by the essential feature of complex permeability not the field distribution effects such as a skin effect.

II. COMPLEX PERMEABILITY

A. Linearized Chua-type model

A Chua-type magnetization model is given by

$$H + (\mu_r/s)dH/dt = (1/\mu)B + (1/s)dB/dt, \quad (1)$$

where H , B , μ , μ_r , and s are the field intensity, flux density, permeability, reversible permeability, and hysteresis coefficient, respectively.¹⁻⁵ To represent the exact magnetization characteristics of the magnetic materials, the parameters μ , μ_r , and s in Eq. (1) must be represented as the functions of flux density, field intensity, and time derivative of flux density. However, these parameters can be assumed to take the constant values when the flux density B as well as field intensity H are sinusoidally time varying. Thus, a linearized Chua-type model is simply derived by assuming the constants μ , μ_r , and s in Eq. (1). When we employ a complex notation $d/dt = j\omega$, then Eq. (1) can be represented by

$$\hat{H} + j\omega(\mu_r/s)\hat{H} = (1/\mu)\hat{B} + j(\omega/s)\hat{B}, \quad (2)$$

where $j = \sqrt{-1}$, $\omega = 2\pi f$ (f : frequency), and the carats refer to complex quantities. By means of Eq. (2), the complex permeability $\hat{\mu}(\omega)$ is defined by

$$\begin{aligned} \hat{\mu}(\omega) &= \hat{B}/\hat{H} = \mu_R(\omega) - j\mu_I(\omega) \\ &= \mu\{(s^2 + \omega^2\mu\mu_r)/(s^2 + \omega^2\mu^2)\} \\ &\quad - j\mu\omega s\{(\mu - \mu_r)/(s^2 + \omega^2\mu^2)\}. \end{aligned} \quad (3)$$

B. Frequency characteristics of the complex permeability

When we take the limits of frequency in Eq. (3), we have

$$\lim_{\omega \rightarrow 0} \mu_R(\omega) = \mu, \quad (4a)$$

$$\lim_{\omega \rightarrow \infty} \mu_R(\omega) = \mu_r, \quad (4b)$$

$$\lim_{\omega \rightarrow 0} \mu_I(\omega) = 0, \quad (4c)$$

$$\lim_{\omega \rightarrow \infty} \mu_I(\omega) = 0. \quad (4d)$$

Consideration of Eqs. (4a) and (4b) reveals that the characteristics in the low- and high-frequency regions are dominated by the permeability μ and reversible permeability μ_r , respectively. In the other words, the parameters μ and μ_r in the linearized Chua-type model (1) can be determined by the low- and high-frequency conditions.

The imaginary part of complex permeability $\mu_I(\omega)$ in Eq. (3) is modified into

$$\begin{aligned} \mu_I(\omega) &= \mu\{\omega(\mu - \mu_r)s/(s^2 + \omega^2\mu^2)\} \\ &= \{\mu(\mu - \mu_r)s\}/\{[\sqrt{\omega}\mu - (s/\sqrt{\omega})]^2 + 2\mu s\}, \end{aligned} \quad (5)$$

so that the maximum value of $\mu_I(\omega)$ is $\mu_I(\omega)|_{\max} = (\mu - \mu_r)/2$, at the frequency $f_I = s/(2\pi\mu)$. Thus, the hysteresis coefficient s in Eq. (1) can be determined by measuring the frequency f_I . The parameters μ , μ_r , and s of a tested ferrite toroidal core, TDK H5c2, are 1.27×10^{-2} H/m, 3.104×10^{-5} H/m, and $54.3 \Omega/\text{m}$, respectively. The frequency characteristics of complex permeability are shown in Fig. 1 together with the experimental results.

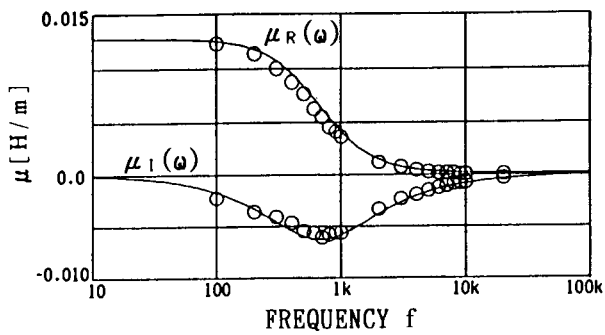


FIG. 1. Frequency characteristics of the complex permeability. Upper: $\mu_R(\omega)$; lower: $\mu_I(\omega)$; solid line: calculated; and circle: measured.

C. Iron loss

By means of the complex permeability $\mu_R(\omega)$, $\mu_I(\omega)$ in Eq. (3), a loss angle $\tan \delta$ can be represented as

$$\begin{aligned} \tan \delta &= \mu_I(\omega) / \mu_R(\omega) \\ &= s(\mu - \mu_r) / \{ [\sqrt{\omega\mu\mu_r} - (s/\sqrt{\omega})]^2 \\ &\quad + 2s\sqrt{\mu\mu_r} \}. \end{aligned} \quad (6)$$

From Eq. (6), we can find that the loss angle $\tan \delta$ takes the maximum value $\tan \delta|_{\max} = (\mu - \mu_r) / (2\sqrt{\mu\mu_r})$, at the frequency $f_t = s / (2\pi\sqrt{\mu\mu_r})$. Figure 2 shows a frequency characteristic of the loss angle $\tan \delta$ calculated by Eq. (6). Obviously, some deviations between the calculated and experimental results are observed in the frequency range 8–20 (kHz). At this frequency range, the permeabilities $\mu_R(\omega)$ obtained by experiments take such small values that the experimental errors are magnified.

The iron loss P_i per unit volume is given by

$$P_i = [B^2\omega^2s(\mu - \mu_r)] / [2\mu(s^2 + \omega^2\mu_r^2)]. \quad (7)$$

This iron loss P_i becomes zero at low frequency $\omega \rightarrow 0$. However, at high frequency, this becomes a constant value $P_i \rightarrow B^2s(\mu - \mu_r) / (2\mu\mu_r^2)$ when the flux density B is held constant. Figure 3 shows the iron loss calculated by Eq. (7) together with the experimental results.

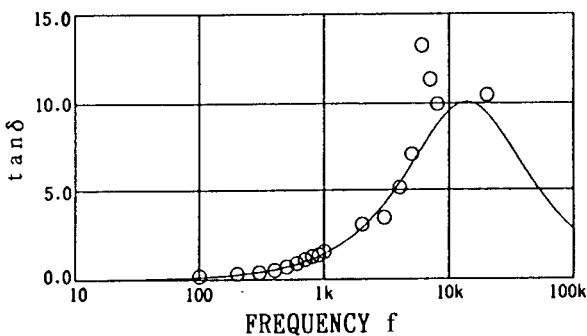


FIG. 2. Frequency characteristic of the loss angle $\tan \delta$. Solid line: calculated; circle: measured.

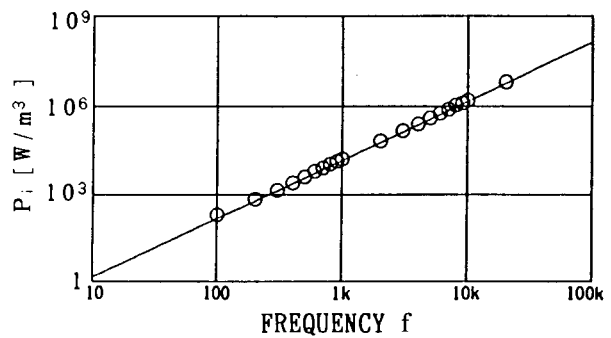


FIG. 3. Frequency characteristic of the iron loss at $B=0.2$ (T). Solid line: calculated; circle: measured.

D. Field distribution

For the case of sinusoidal B and H , Maxwell's equations yield the complex Helmholtz relation:

$$\nabla^2 \hat{B} + \hat{\alpha} \hat{B} = 0, \quad (8a)$$

$$\hat{\alpha} = \omega\kappa\mu [(\omega\mu_r - js) / (s + j\omega\mu)], \quad (8b)$$

whose solution may be obtained by the finite-element method.⁶ A problem region is a cross section of the tested ferrite core having conductivity $\kappa = 6.667$ s/m and cross sectional 1×1 cm².

A boundary condition at the interface between the exciting coil and core is $\hat{H}|_{\text{coil}} = \hat{B} / \hat{\mu}(\hat{\omega})|_{\text{core}}$. From the FEM solutions, it has been found that the magnetic field is uniformly distributed over the cross section of tested core under the 1-, 3-, and 10-kHz exciting conditions. Nevertheless, observed hysteresis loops in Fig. 4 take the different loops according to the operating frequencies. Examination of the results in Figs. 1 and 4 obviously suggests that the frequency dependence of observed hysteresis loops is mainly dominated by the essential frequency character-

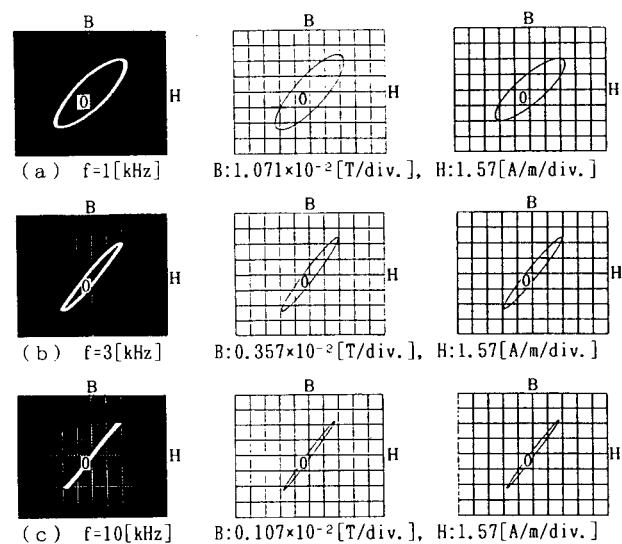


FIG. 4. Observed hysteresis loops. Left: measured; middle: calculated by lumped circuit model; and right: calculated by FEM. (a) 1, (b) 3, and (c) 10 (kHz).

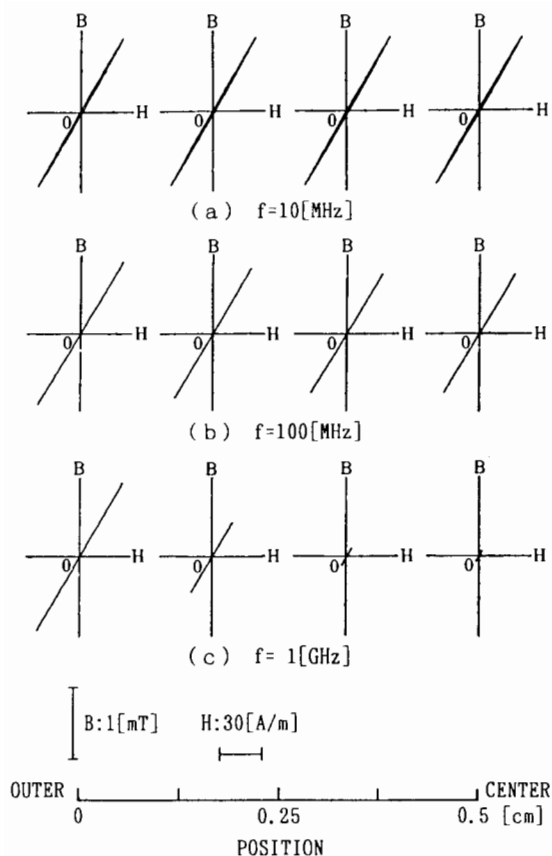


FIG. 5. Hysteresis loops along a diagonal line of the tested core cross section.

istic of complex permeability not the field distribution effects such as a skin effect. As shown in Fig. 5, the field distribution effect due to hysteresis can be observed at the higher frequencies.

III. CONCLUSIONS

We have derived a complex permeability from the linearized Chua-type magnetization model and clarified the frequency characteristics of the complex permeability as well as iron loss. Further, it has been shown that the frequency characteristic of the observed hysteresis loops are mainly dominated by the essential features of the complex permeability not the field distribution effects. It should be noted that our analysis is valid when the flux density is sufficiently small that it varies sinusoidally in response to the sinusoidal field intensity. Also, similar analysis and experiments are given in Ref. 7.

¹Y. Saito, S. Hayano, Y. Kishino, K. Fukushima, H. Nakamura, and N. Tsuya, *IEEE Trans. Magn.* **MAG-22**, 647 (1986).

²Y. Saito, K. Fukushima, S. Hayano, and N. Tsuya, *IEEE Trans. Magn.* **MAG-23**, 2227 (1987).

³Y. Saito, S. Hayano, and Y. Sakaki, *J. Appl. Phys.* **64**, 5684 (1988).

⁴Y. Saito, M. Namiki, and S. Hayano, *IEEE Trans. Magn.* **MAG-25**, 2968 (1989).

⁵Y. Saito, M. Namiki, and S. Hayano, *J. Appl. Phys.* **67**, 4738 (1990).

⁶P. P. Silvester and R. L. Ferrari, *Finite Elements for Electrical Engineers* (Cambridge University, Cambridge, 1983).

⁷E. C. Snelling, *Soft Ferrites, Properties and Applications* (ILIFFE Books, London, 1969).